**SUPPLEMENTARY INFORMATION**

## DETAILED METHODS

### *Mouse genotyping*

C3H/HeSnJ and *Slc35d3*$^{ros/ros}$ mice were genotyped by PCR using the following primers designed to detect the insertional mutation in the *Slc35d3* gene[23]: forward primer 1, CATCCTTCTGACCCAGGAAC; forward primer 2, GTGACGGCGAATGTGGG; reverse primer, CGATGAGCATGGTGACTAGG. A 708 bp fragment is amplified from the wt *Slc35d3* gene using forward primer 1 and the reverse primer, whereas a 356 bp fragment is amplified from the *Slc35d3*$^{ros/ros}$ gene using forward primer 2 and the reverse primer. Homozygous *pallid* (*Pldn*$^{pa/pa}$) and *pearl* (*Ap3b1*$^{pe/pe}$) mice were identified by their coat color, and homozygous *light ear* (*HPS4*$^{le/le}$) mice were identified by the loss of pigmentation in the tail and ears.

### *Antibodies used in Supplementary Figures*

Rabbit monoclonal antibodies to RAB5, RAB7 and RAB11 were purchased from Cell Signaling Technology (Danvers, MA). Rabbit polyclonal antibody to Giantin was from Abcam. Rabbit polyclonal antibody to *trans* Golgi p230/ tGolin-1 (TG-p230) was as described [51].

### *Recombinant DNA procedures*

To make epitope-tagged *SLC35D3* constructs, a full-length human *SLC35D3* cDNA in a pCMV-SPORT6 vector was purchased from ATCC (Washington, DC). A *BamH*I cloning site, Kozak consensus translation start sequence, an N-terminal HA11 epitope tag and a downstream *Xba*I cloning site were incorporated by PCR amplification of the cDNA, and then the modified *BamH*I-

*Xba*I fragment was subcloned into pCDM8.1[52] to generate pCDM8.1-HA-SLC35D3. The ensuing *Sal*I-*Not*I fragment encompassing the HA-SLC35D3 coding sequence was then subcloned into the *Xho*I and *Not*I sites of retroviral vector pBMN-IRES(X/N)-hygro[15]. To generate SLC35D3 with a C-terminal HA11 tag (SLC35D3-HA), an upstream *BamH*I site and downstream sequence encoding HA11 epitope followed by a stop codon and *Not*I site were created by PCR amplification of the full-length SLC35D3 in pCDM8.1 and then subcloned into pBMN-IRES(X/N)-hygro. To generate SLC35D3 with an N-terminal myc-epitope tag, full-length SLC35D3 cDNA with an upstream *BamH*I site and sequence encoding a Kozak consensus sequence and Myc tag and down stream *Not*I site were generated by PCR amplification, then subcloned into the *BamH*I and *Not*I sites of pBMN-IRES(X/N)-hygro. To generate an expression vector for untagged mouse SLC35D3, a full-length mouse *Slc35d3* cDNA in the pFLC1 vector was purchased from Source BioScience LifeSciences (Berlin, Germany), and the cloning region was amplified by PCR and subcloned into pBMN-IRES(X/N)-hygro as described above for human HA-*SLC35D3*. All constructs were verified by DNA sequencing. Details of primers used in generating the tagged forms are available upon request.

***Platelet isolation***

Blood was drawn from the inferior vena cava of anesthetized mice into a 1 ml syringe containing 0.2 ml ACD buffer (85 mM trisodium citrate, 71.4 mM citric acid, 11.1 mM dextrose, pH 4.9). The blood was adjusted to a volume of 3 ml by slowly adding and gently mixing with wash buffer (134 mM NaCl, 3 mM KCl, 0.3 mM $NaH_2PO_4$, 2 mM $MgCl_2$, 5 mM HEPES, 5 mM glucose, 1 mg/ml albumin, 1% $NaHCO_3$ and 1 mM ethylene glycol-bis (2-aminoethylether)-N,N, N',N'-tetraacetic acid, pH 7.2), and then centrifuged at 13*g* for 5 minutes at RT to collect platelet rich plasma (PRP). Prostaglandin E1 (PGE1) was added to the PRP to a final concentration of 0.5

μM to prevent platelet activation, and then platelets were pelleted by centrifugation at 62*g* for 10 minutes at RT.

**Immunofluorescence microscopy and measurement of colocalization.** The DM IRBE microscope used was equipped with a 63X Plan Apo lens (1.4 NA), motorized focus drive and narrow band pass filters to detect FITC/ Alexaflour 488/ mepacrine, Texas Red/ Alexafluor 594, and Hoechst 33342 with no overlap, as verified by samples labeled individually for a single chromophore. The cells analyzed had no appreciable autofluorescence, as detected from unstained samples using comparable exposure and gain settings to those used to capture the images that were analyzed, and the secondary antibodies used in double labeling experiments were species or isotype-specific as shown by a lack of cross-reactivity in experiments in which cells were labeled with both primary antibodies and a single secondary antibody. Images from sequential z-planes were captured in 200 nm intervals, as recommended by the software and hardware manufacturers. Iterative volume deconvolution for each z-series stack was performed using Volocity software (v. 5.3) on partially cropped images, ensuring that the cell to be analyzed occupied less than 40% of the space. Colocalization was quantified from 3-dimensional reconstructions of deconvolved images using Volocity software, and is presented as a thresholded Pearson's correlation coefficient from at least five cell profiles for each pairwise comparison. Threshold levels for each channel in each image were determined by choosing several areas of blank space in the image using the "voxel pick tool" and calculating the average intensity of the signals. Saturated signals were also excluded from the analysis using the same procedure. Deconvolved images are shown in the extended focus mode in order to account for the tubular shape of most early endosomes and to thus allow for visualization of adjacent early endosomal domains. Single deconvolved z-plane images, in which such domains are often segregated resulting in a more punctate appearance, are shown

in Supplementary Figure S3 along with x-z and x-y plane images that demonstrate the adjacent domains.

In our analyses of differentiating G1ME cells, the cells had various sizes, likely due to asynchronous differentiation and perhaps to differential expression of the GATA-1 transgene. Only cells with multiple nuclei were analyzed. The largest cells were typically excluded because they overexpressed the SLC35D3 transgene (as indicated by fluorescence signal throughout the cytoplasm even at low exposures), and cells with single nuclei – which largely represent either undifferentiated G1ME cells that were not transduced with GATA-1 or cells that differentiated toward the erythroid lineage – were also excluded. Among the remaining multinucleated cells, no significant differences in transgene colocalization were observed for any given marker pair, regardless of cell size (p values ranged from 0.18 to 0.86).

**SUPPLEMENTARY REFERENCES**

51. Yoshino A, Setty SRG, Poynton C, et al. tGolgin-1 (p230, golgin-245) modulates Shiga-toxin transport to the Golgi and Golgi motility towards the microtubule-organizing centre. *J Cell Sci*. 2005;118:2279-2293.

52. Bonifacino JS, Suzuki CK, Klausner RD. A peptide sequence confers retention and rapid degradation in the endoplasmic reticulum. *Science*. 1990;247:79-82.

**SUPPLEMENTARY TABLE 1: Primers used for real-time qPCR analysis**

| Gene | Sequence (5' to 3') | Direction |
|---|---|---|
| Slc35d3 | GGACCCGGCCATGGTT | Sense |
| | CATGGCACAGCCGATCAG | Anti-sense |
| MRP4 | AAAGCTGCATCGGGAAGCT | Sense |
| | CCGTGAAAGCCGCAGTTT | Anti-sense |
| GAPDH | GAAGGTACGGAGTCAACGGATTT | Sense |
| | GAATTTGACCATGGGTGGAAT | Anti-sense |

**Supplementary Movies**

**Supplementary Movie 1**: Three-dimensional reconstruction of IFM analysis of transduced G1ME cells labeled for HA-SLC35D3 and mepacrine. See legend to **Supplementary Figure S3**.

**Supplementary Movie 2**: Three-dimensional reconstruction of IFM analysis of transduced G1ME cells labeled for HA-SLC35D3 and STX13. See legend to **Supplementary Figure S3**.

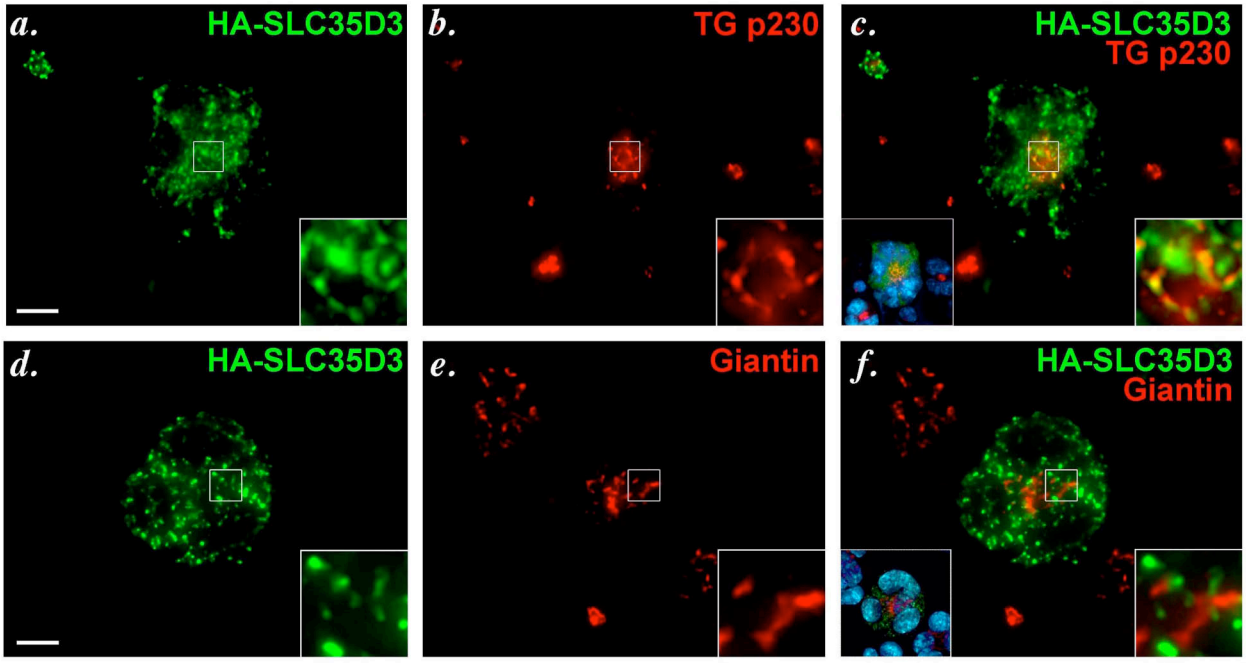


**Supplementary Figure S1. HA-SLC35D3 does not accumulate in Golgi-associated structures.** G1ME cells were doubly infected with recombinant retroviruses expressing GATA-1 and HA-SLC35D3 and large multinucleated cells were analyzed 4 days post-infection by deconvolution IFM as in Figures 2 and 3 after labeling for HA-SLC35D3 (green), for markers of the TGN (*a*-*c*) or the early Golgi (*d*-*f*) (red), and for nuclei (blue). HA-SLC35D3 (*a*, *d*) was labeled with anti-HA antibody, the TGN with anti-trans Golgi p230 antibody (TG p230; *b*), and the Golgi with anti-giantin antibody (*e*). Overlays are shown in *c* and *f*, right insets show a 5-fold magnification of the boxed region, and the left insets in *c* and *f* show overlays of non-deconvolved images with nuclei labeled in blue. Note the overlap of HA-SLC35D3 and TG p230 in the pericentriolar region, but the majority of HA-SLC35D3 labeling in the periphery does not label for TGN or Golgi. Scale bar, 10 μm.

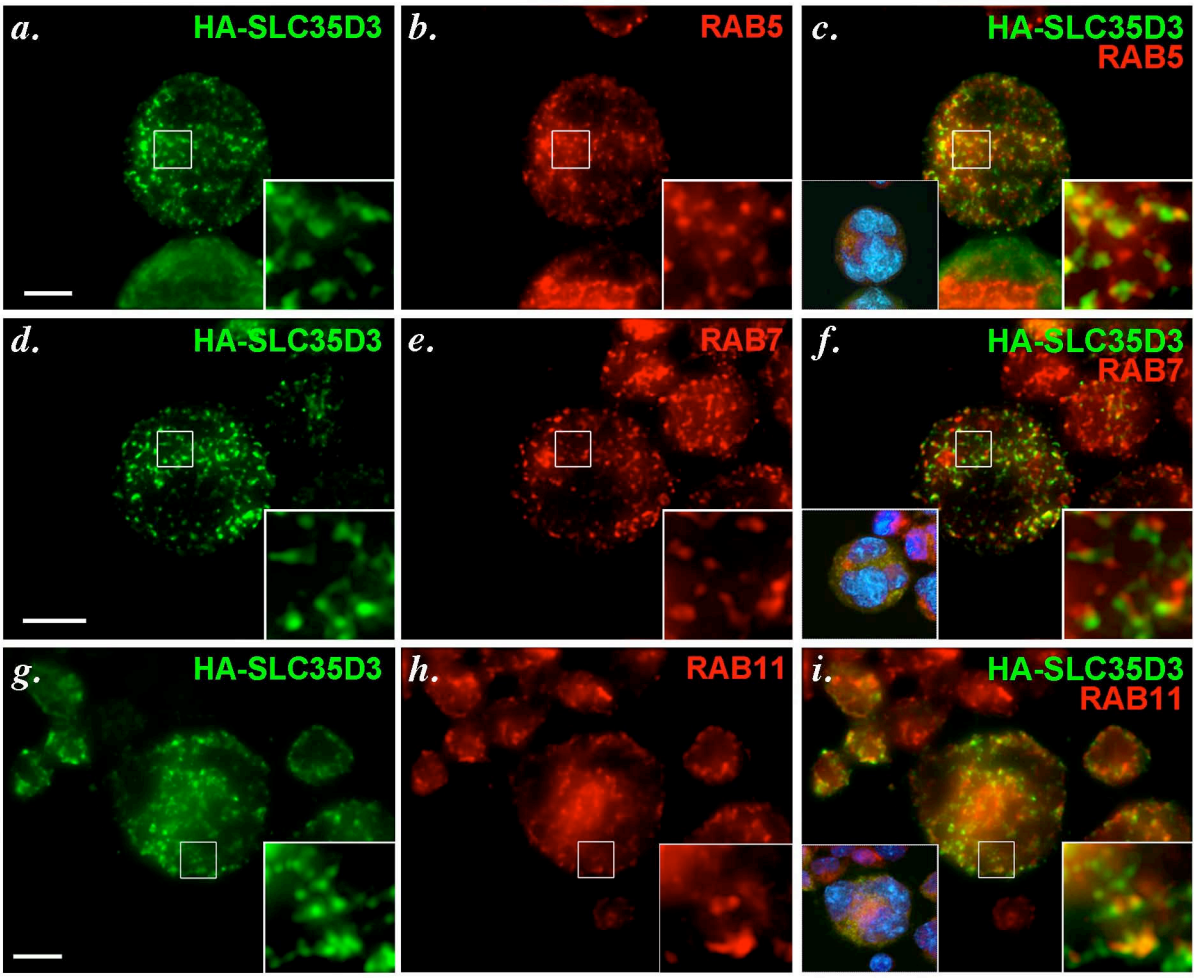


**Supplementary Figure S2. Overlap of HA-SLC35D3 with endosomal Rab proteins in G1ME cells.** G1ME cells were doubly infected with recombinant retroviruses expressing GATA-1 and HA-SLC35D3 and large multinucleated cells were analyzed 4 days post-infection by deconvolution IFM as in Figures 2 and 3 after labeling for HA-SLC35D3 (green), for the endosomal RAB proteins (red) RAB5 (*a-c*; early sorting endosomal domains), RAB7 (*d-f*; late endosomal domains) or RAB11 (*g-i*; early recycling endosomal domains), and for nuclei (blue). Overlays are shown in *c*, *f* and *i*; right insets show a 5-fold magnification of the boxed regions; and the left insets in *c*, *f* and *i* show overlays of non-deconvolved images with nuclei labeled in blue. Scale bar, 10 μm.

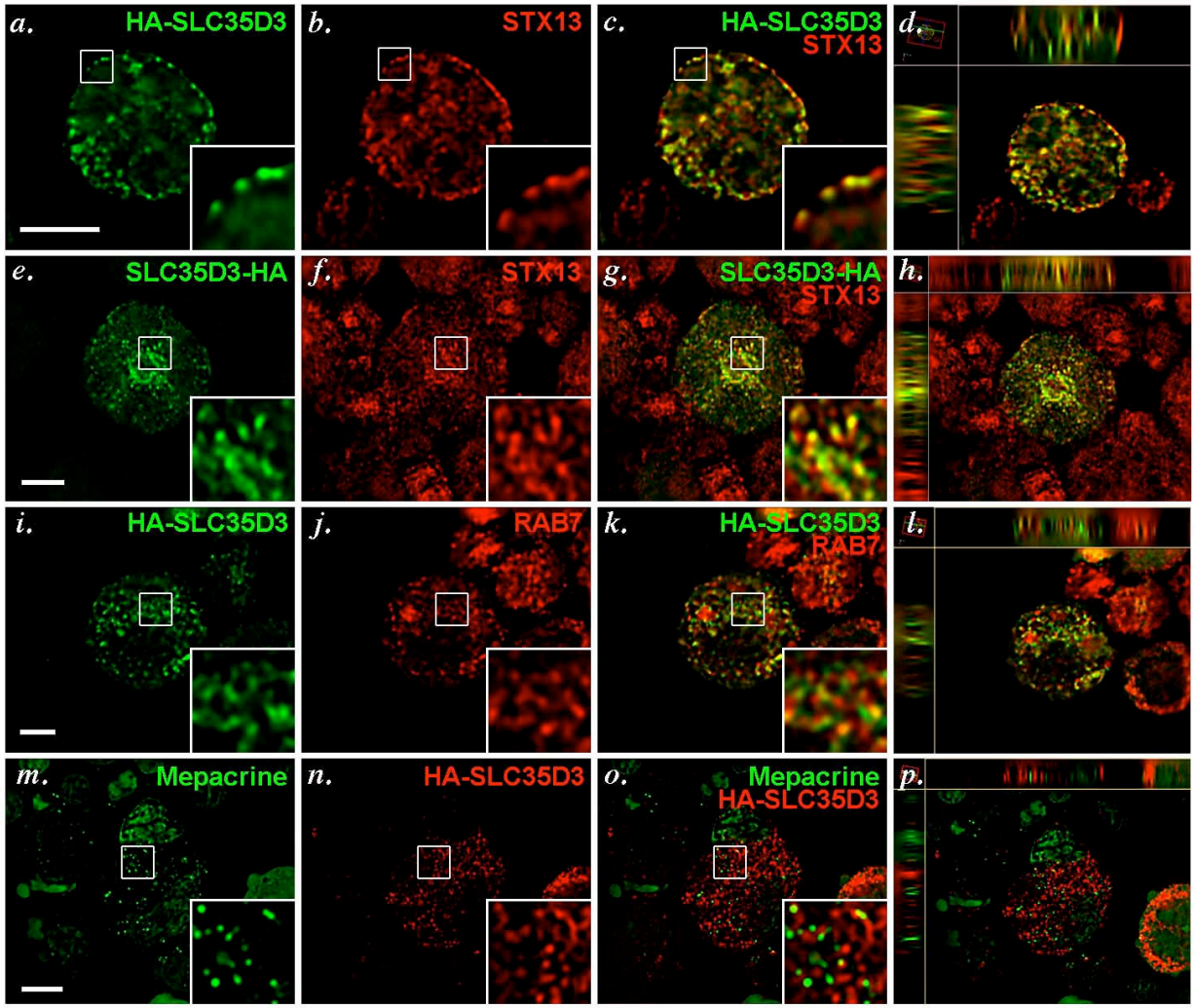


**Supplementary Figure S3. HA-SLC35D3 is present in endosomal domains that are adjacent to and continuous with STX13-containing domains.** G1ME cells were doubly infected with recombinant retroviruses expressing GATA-1 and HA-SLC35D3, and large multinucleated cells were analyzed 4 days post-infection by deconvolution IFM. Cells were immunolabeled for: *a*-*d*, HA-SLC35D3 (green) and STX13 (red); *e*-*h*, SLC35D3-HA (green) and STX13 (red); *i*-*l*, HA-SLC35D3 (green) and RAB7 (red); or *m*-*p*, HA-SLC35D3 (red) after uptake of mepacrine (green). Shown are representative single plane x-y plane images alone (*a*-*c*, *e*-*g*, *i*-*k*, *m*-*o*) or with x-z (top) and y-z (left) images (*d*, *h*, *l*, *p*) after 3-dimensional reconstruction of deconvolved stacks. Insets show 5X magnifications of the boxed regions. Cells analyzed are

the same as those shown in extended focus mode in Fig. 3*a*-*c*, Fig. 3*d*-*f*, Suppl. Fig. S2*d*-*f*, and Fig. 2*d*-*f*, respectively. Note the distortion in the z-axis in panels *d*, *h*, *l* and *p*.

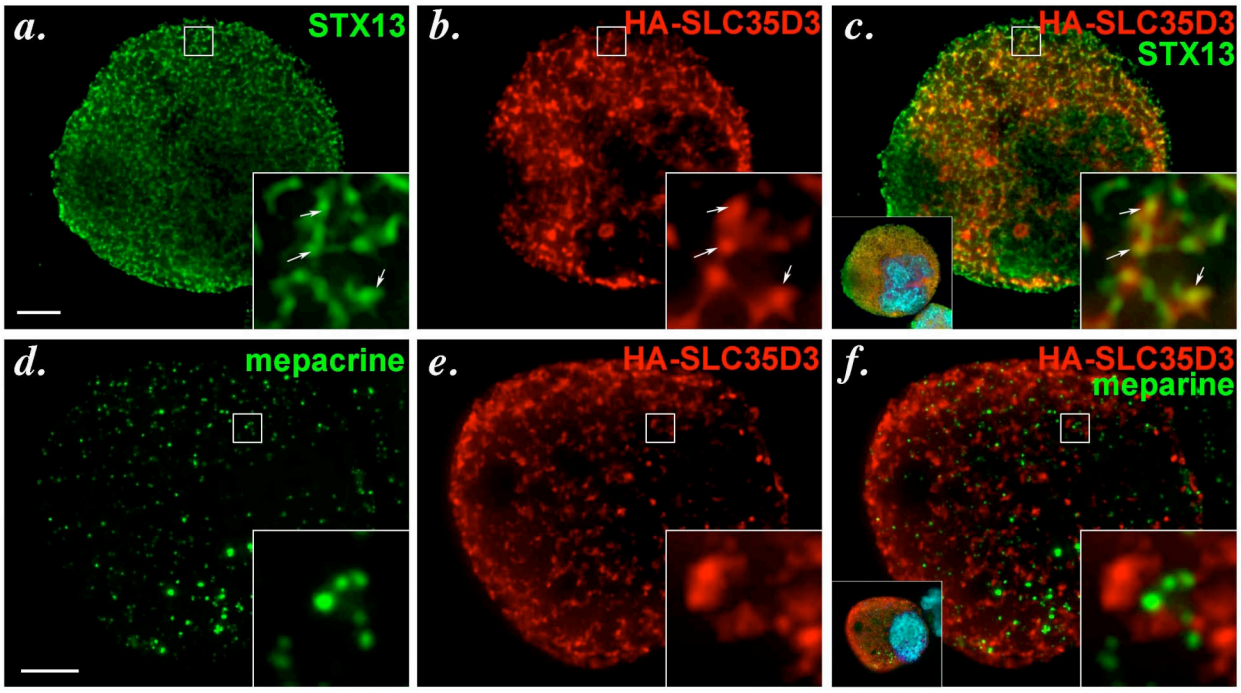


**<u>Supplementary Figure S4.</u> SLC35D3 localizes to early endosomes in primary MKs.** Fetal liver cells were infected with recombinant retrovirus expressing SLC35D3-HA and cells were analyzed 8 days later after culture with Tpo. Deconvolution IFM was used as in Figures 2 and 3. Top panel (***a-c***): HA-SLC35D3 (green) was labeled with anti-HA and early endosomes (red) were labeled with antibodies to STX13. Bottom panel (***d-f***): HA-SLC35D3 (red) was labeled with anti-HA and DGs were labeled with mepacrine (green). Insets, 5-fold magnification of the boxed region to emphasize the red and green signal. Scale bar, 10 μm.

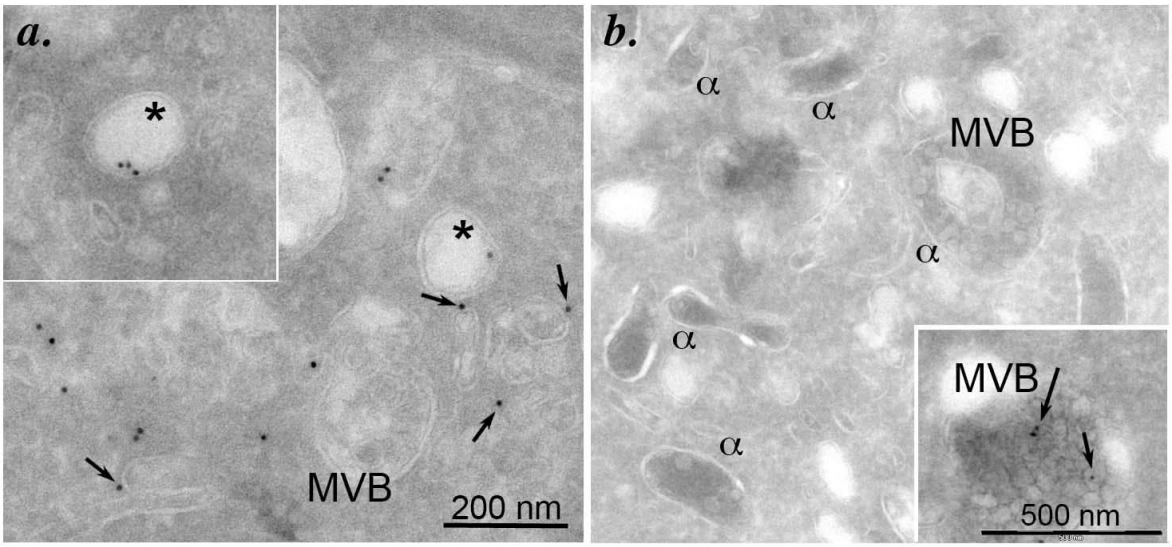


**<u>Supplementary Figure S5.</u> SLC35D3 accumulates in structures with ultrastructural characteristics of early endosomes in G1ME cells.** Ultrathin cryosections of G1ME cells that had been doubly transduced by GATA-1 and HA-SLC35D3 retroviruses were immunogold labeled with anti-HA antibody and 10 nm protein A gold particles. *a.* Gold particles were predominantly found in tubulovesicular structures (arrows), often in close proximity to multivesicular bodies (MVB) and immunogold labeled vacuolar endosomal domains (asterisks). Inset: labeling in a representative vacuolar endosome. *b.* A field from the same cell showing abundant structures with characteristics of $\alpha$-granules ($\alpha$) and a multivesicular body (MVB) that were not immunogold labeled. Inset: immunogold labeling of SLC35D3 (arrows) within a MVB.

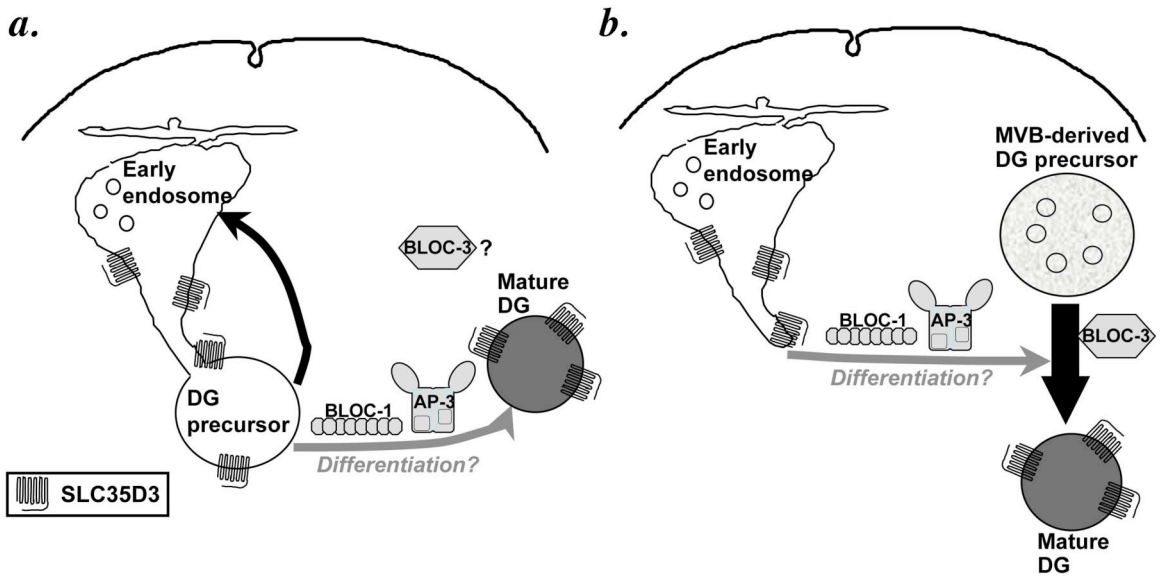


**Supplementary Figure S6. Two models of cargo delivery to dense granules from early endosomes in MKs and platelets.** *a*. In the first model, the membranes of early endosomes and DG precursors are in a constant dynamic equilibrium in MKs. The small surface area of DGs relative to the early endosomal system would favor detection of SLC35D3 on endosomes in MKs. Upon differentiation to proplatelets, the DG precursors mature and segregate from early endosomes in a process requiring BLOC-1 and AP-3 but not BLOC-3. *b.* In the second model, cargoes such as SLC35D3 are retained in early endosomes in immature MKs, and are delivered to precursors that are derived from multivesicular bodies (MVB) upon differentiation into proplatelets in a process requiring BLOC-1 and AP-3. In this model, the formation of the precursors or the delivery of separate cargoes to those precursors requires BLOC-3.